ANTICANCER RESEARCH *42*: 5719-5729 (2022)
doi:10.21873/anticanres.16079

GPX4 Regulates Tumor Cell Proliferation *via* Suppressing Ferroptosis and Exhibits Prognostic Significance in Gastric Cancer

KEN SUGEZAWA[1], MASAKI MORIMOTO[1], MANABU YAMAMOTO[1], YOSHIAKI MATSUMI[2], YUJI NAKAYAMA[3], KAZUSHI HARA[1], CHIHIRO UEJIMA[1], KYOICHI KIHARA[1], TOMOYUKI MATSUNAGA[1], NARUO TOKUYASU[1], TERUHISA SAKAMOTO[1], YOSHIHISA UMEKITA[4] and YOSHIYUKI FUJIWARA[1]

[1]*Division of Gastrointestinal and Pediatric Surgery, Department of Surgery, Faculty of Medicine, Tottori University, Yonago, Japan;*
[2]*Division of Chemical Biology, Technical Department, Tottori University, Yonago, Japan;*
[3]*Division of Radioisotope Science, Research Initiative Center, Organization for Research Initiative and Promotion, Tottori University, Yonago, Japan;*
[4]*Division of Organ Pathology, Department of Pathology, Faculty of Medicine, Tottori University, Yonago, Japan*

Abstract. *Background/Aim: Gastric cancer (GC) is the fourth leading cause of cancer-related death worldwide. Glutathione peroxidase 4 (GPX4) is a glutathione-dependent antioxidant enzyme known to regulate ferroptosis, which is a non-apoptotic form of cell death accompanied by iron-dependent accumulation of reactive oxygen species (ROS). This study evaluated the expression and function of GPX4 in GC. Materials and Methods: The expression of GPX4 was examined in five human GC cell lines (KATO-III, MKN-1, MKN-28, MKN-45, and MKN-74) using real-time quantitative PCR and western blotting. The role of GPX4 in GC was examined using small interference RNA and cell proliferation and ROS assays. Finally, we analyzed GPX4 expression in tumor tissues from 106 patients who underwent GC surgery using immunohistochemistry and evaluated the relationship between GPX4 levels and clinical outcomes of GC. Results: GPX4 was expressed in all GC cell lines at various levels. GPX4 silencing and inhibition significantly reduced cell proliferation and increased ROS generation. Furthermore, the mRNA levels of prostaglandin-endoperoxide synthase 2, a known biomarker of ferroptosis, were increased after GPX4 silencing. GPX4 expression was found to be an independent prognostic factor for overall and disease-specific survival in GC patients. Conclusion: GPX4 can regulate cancer cell death via ferroptosis in GC cell lines and represents a significant risk factor for survival in patients with GC.*

Correspondence to: Masaki Morimoto, Department of Surgery, Division of Gastrointestinal and Pediatric Surgery, Faculty of Medicine, Tottori University, 36-1 Nishi-cho, Yonago 683-8504, Japan. Tel: +81 859386567, e-mail: 2s.morimoto@gmail.com

Key Words: GPX4, ferroptosis, gastric cancer, reactive oxygen species.

Gastric cancer (GC) is the fourth leading cause of cancer-related death worldwide (1). Advances in screening programs, endoscopic resection, surgery, and chemotherapy, including peri/postoperative chemotherapy, have improved the prognosis of patients with GC. If treated early, the current 5-year overall survival (OS) rate for GC is >90% (2).

Recently, emerging cancer mechanisms and targeted compounds have provided novel therapeutic strategies for advanced or metastatic GC patients, such as the blockade of human epidermal growth factor receptor 2 and/or immune checkpoint proteins. However, satisfactory outcomes for patients with advanced GC have not yet been achieved. Therefore, further investigation of oncogenic mechanisms in GC and development of novel targeted therapies are needed.

Glutathione peroxidase 4 (GPX4) is a glutathione-dependent antioxidant enzyme that can directly reduce phospholipid hydroperoxides generated by the oxidation of membrane phospholipids and is a selenoprotein with selenocysteine in its active site (3). It has been shown that disorders of cell death systems can induce malignancies (4). GPX4 is known to be a regulator of ferroptosis, which is defined as non-apoptotic cell death accompanied by iron-dependent accumulation of reactive oxygen species (ROS) (5). In cancer tissues, GPX4 is highly expressed in hepatocellular carcinoma (6) and colorectal carcinoma (7), whereas it is down-regulated in breast cancer (8) and renal cell carcinoma (9) compared with normal tissues.

In diffuse large B-cell lymphoma (10), lung adenocarcinoma (11), and esophageal cancer (12), the degree of GPX4 expression has been reported to be related to prognosis and has attracted attention as a prognostic factor. Nevertheless, there are few studies that have determined whether the expression of GPX4 has a prognostic role in patients with GC. Furthermore, detailed mechanisms and the role of ferroptosis in tumor progression remain unclear, especially for GC. Therefore, in this study, we evaluated the expression and function of GPX4 in GC cell lines and the prognostic significance of GPX4 expression in surgically resected cancer specimens from advanced GC patients.

Materials and Methods

Cell culture. The expression of GPX4 was examined in five human GC cell lines: MKN-1, MKN-45, and MKN-74, which were purchased from the Riken Cell Bank (Tsukuba, Japan); and KATOIII and MKN-28 cells, which were kindly provided by Prof. Hisao. Ito (Division of Organ Pathology, Tottori University, Yonago, Japan). All of the cell lines were cultured in Roswell Park Memorial Institute medium (RPMI 1640; FUJIFILM Wako Pure Chemical Co., Osaka, Japan) supplemented with 10% fetal bovine serum (Cosmo Bio Co., Ltd, Tokyo, Japan). The cells were maintained at 37˚C in atmospheric air supplemented with 5% carbon dioxide and passaged at a ratio of 1:3-1:10 every 3-5 days.

RNA isolation and quantitative RT-PCR analysis. Cells were seeded in 6-well plates with three independents samples per each group. All RNA preparation and handling steps were performed under RNAse-free conditions. Total RNA was isolated using PureLink RNA Mini Kit (Thermo Fisher Scientific, Waltham, MA, USA), according to the manufacturer's instructions. Briefly, 1 ml of TRI reagent (Molecular Research Center, Inc., Cincinnati, OH, USA) was added per well. After thoroughly pipetting, 200 μl of chloroform was added and centrifuged at 12,000×*g* for 15 min at 4˚C. The aqueous layer was collected, an equal volume of 70% EtOH was added, vortexed, applied to the Spin Cartridge, centrifuged at 12,000×*g* for 40 s at room temperature, the flow-through discarded, Wash Buffer I applied, and the sample centrifuged at 12,000×*g* for 20 s at room temperature. After the tube was renewed, Wash Buffer II is applied and centrifuged at 12,000×*g* for 20 s at room temperature. After centrifugation at 12,000×*g* for 2 min, RNA concentration was measured by a Nano-drop (Thermo Fisher Scientific) to determine the amount required for 1 μg of total RNA.

After isolation, cDNA synthesis was performed using SuperScript IV VILO Master Mix (Thermo Fisher Scientific) in a total volume of 20 μl according to the manufacturer's instructions. Reverse transcription was performed using a Thermal Cycler (Hangzhou Bioer Technology Co. Ltd., Hangzhou, PR China) at 25˚C for 10 min, 50˚C for 10 min, and 85˚C for 5 min.

The cDNAs were then subjected to quantitative PCR analysis with TaqMan Gene Expression Assay probes and TaqMan Fast Advanced Master Mix premixed with ROX on a ViiA7 system (Applied Biosystems, Pleasanton, CA, USA) using the following conditions: 50˚C for 2 min, 95˚C for 20 s, and 40 cycles of 95˚C for 1 s and 60˚C for 20 s. Primers and probes were used without modification. The negative control had no template. Quantification was performed with the ΔΔCT method. Quantitative results were analyzed and presented as fold change. The software used was SDS v1.1. Taqman probes and primers for qPCR were purchased from Applied Biosystems and included those for glutathione peroxidase 4 (GPX4; Hs00989766_g1), prostaglandin-endoperoxide synthase (PTGS2; Hs00153133_m1), and actin beta (ACTB; Hs99999903_m1). Results were calculated by Student *t*-test and expressed using standard deviation.

Western blotting analysis. Cells were seeded in 6-cm dishes. The cells were lysed in RIPA buffer (Nakalai Tesque, Kyoto, Japan). Centrifugation was performed at 21,400×*g* for 10 min at 4˚C, and the supernatants were collected. Protein concentrations were determined using a Bradford Protein Assay (Takara Bio Inc., Shiga, Japan). Proteins were separated by 12% sodium dodecyl sulfate–polyacrylamide gel electrophoresis and then transferred onto 0.2 μm polyvinylidene fluoride membranes (Bio-Rad Laboratories Inc., Hercules, CA, USA). After blocking with 2% ECL Prime Blocking Reagent (Cytiva, Tokyo, Japan), the membranes were incubated with a primary antibody against GPX4 (1:2,000; ab125066; Abcam, Cambridge, UK). A primary antibody against ACTB (1:2,000; sc-47778; Santa Cruz Biotechnology, Dallas, TX, USA) was used for normalization. Peroxidase-conjugated anti-mouse and anti-rabbit secondary antibodies (Cytiva) were used to detect target protein-antibody binding. The protein signals were detected with ECL Prime Western blotting detection reagents (Cytiva) and quantified using the Image Quant LAS 4000 Mini (GE Healthcare, Chicago, IL, USA). The intensity of the proteins was compared using ImageJ software and experiments were performed in triplicate.

Gene silencing of GPX4 using siRNA. The Silencer Select small interference RNA (siRNA) targeting the *GPX4* gene (s6111, s6112; Thermo Fisher Scientific) and a non-silencing siRNA control (sc-37007, Santa Cruz Biotechnology) were purchased. Cells were transfected using Lipofectamine RNAiMAX (Thermo Fisher Scientific). In accordance with the manufacturer's protocol, 5 pmol Silencer Select siRNA, 50 μl of Opti-MEM (Invitrogen, Carlsbad, CA, USA), and 1.5 μl Lipofectamine RNAiMAX transfection reagent were mixed and incubated for 15 min at room temperature. Fifteen μl of the mixture was added to the cells. Control cells were transfected with an equivalent amount of control siRNA. The effect of mRNA silencing was confirmed by qPCR analysis and western blotting.

Cell proliferation assay. Cells were seeded in 96-well plates and incubated overnight. Next, the cells were transfected using *GPX4*-specific siRNA or non-silencing siRNA control reagent. After a 72-h incubation, a 10% v/v of Cell Counting Kit-8 solution (WST assay; DOJINDO, Tokyo, Japan) was added to each well and incubated for 1 h. Absorbance was measured using the Infinite F50 microplate reader (TECAN, Kawasaki, Japan) set at 450 nm/620 nm, and the cell proliferative capacity was assessed. In case of using RSL3, cells were seeded in 96-well plates and incubated overnight. Next, cells were treated with DMSO (0.4%) or RSL3 (10 μM) and after 48 h, the same experiment as described above was performed.

ROS assay. Cells were seeded in 96-well black sided, clear bottom plates (Corning, Corning, NY, USA) and incubated overnight. Cells were transfected using *GPX4*-specific siRNA or non-silencing siRNA control reagent. After a 72-h incubation, the medium was removed, and cells were washed with Hanks' Balanced Salt Solution

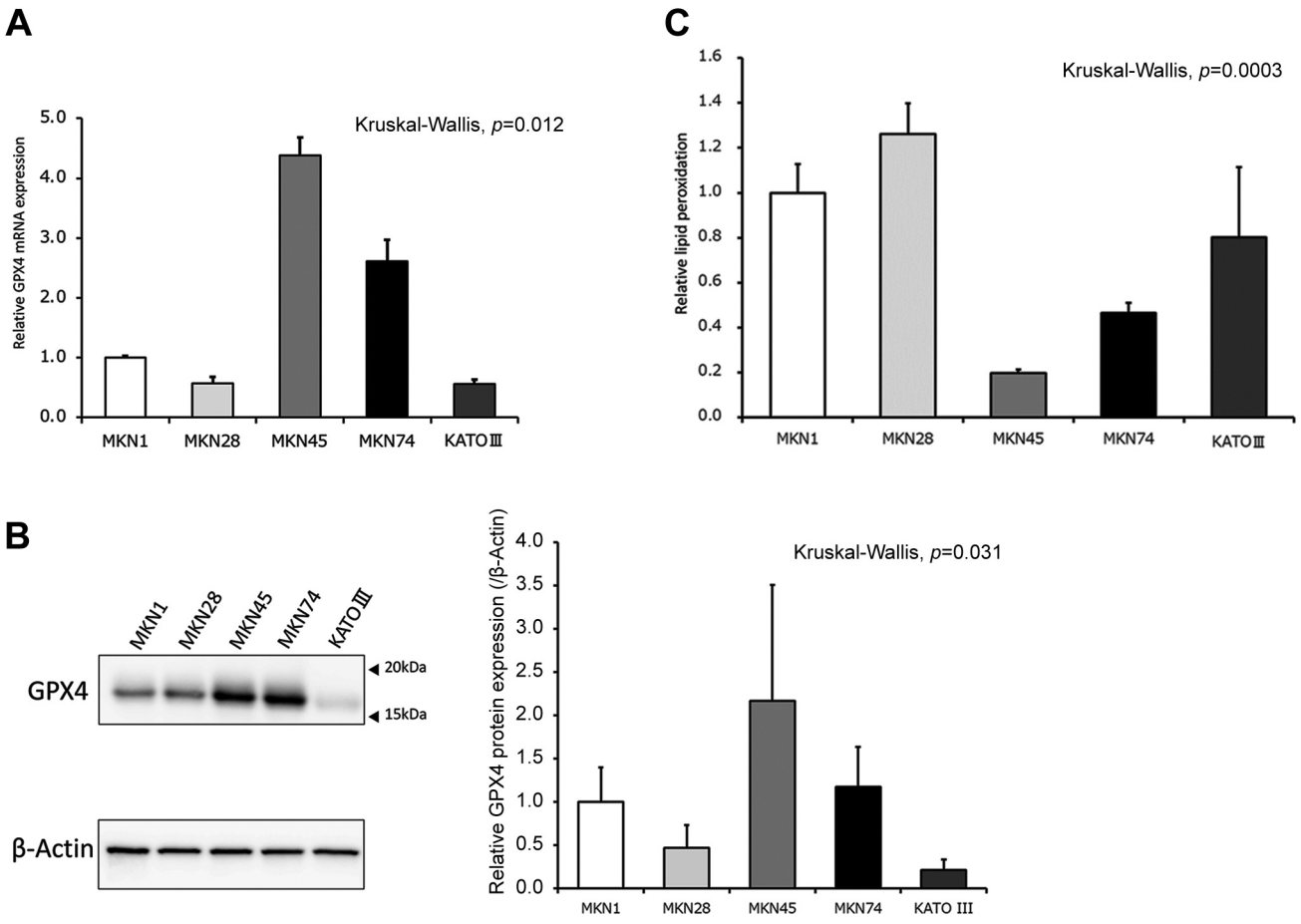

Figure 1. *Continued*

(HBSS) (FUJIFILM Wako Pure Chemical Co.). Highly Sensitive DCFH-DA Dye (DOJINDO) was added to each well (0.1 μl/well) and incubated for 30 min after which the medium was removed, and the cells were washed with HBSS. The fluorescent intensity was measured with an Infinite F500 fluorescence plate reader (TECAN) set at 485 nm excitation and 535 nm emission, and the ROS activity was assessed.

Lipid peroxidation assay. Cells were seeded at 1×10^6 cells in 10-cm dishes. After 72 h, 1×10^6 cells were resuspended in 500 μl of HBSS containing C11-BODIPY (581/591) (0.5 μM) and incubated for 30 min at 37˚C. Cells were then washed with PBS and resuspended in 500 μl HBSS containing DAPI (DOJINDO) (0.5 μl) and analyzed by flow cytometry using BD LSR Fortessa (BD Biosciences, San Jose, CA, USA). In case of using RSL3, cells were seeded at 1×10^6 cells in 10-cm dishes and incubated overnight. Next, cells were treated with DMSO (0.4%) or RSL3 (10 μM). After 48 h, analysis was performed by flow cytometry.

Patients and tumor specimens. Specimens were obtained from 106 consecutive patients who underwent curative gastric resection at the Tottori University Hospital between June 2004 and December 2011. They were classified as Stage II or III according to the 8th Edition of the Union for International Cancer Control-TNM classification. Patients who underwent re-resection for residual cancer were excluded. This study was approved by the institutional review board of Tottori University (No. 20A080).

Immunohistochemical analysis. Immunohistochemistry was performed according to standard protocols. Briefly, formalin-fixed, paraffin-embedded tissue was processed into 4-μm thick sections. After deparaffinizing the tissue blocks, antigens were retrieved by autoclaving at 121˚C for 10 min in Histofine (pH 9.0; Nichirei Biosciences Inc., Tokyo, Japan). Endogenous peroxidase in the tissue sections was blocked by incubation with 3% hydrogen peroxide for 30 min, and non-specific protein binding was blocked with 10% Block-Ace (DS Pharma Biomedical, Osaka, Japan) for 30 min. Anti-GPX4 (ab125066; Abcam) was used at the dilution of 1:200. Specimens were incubated with primary antibody overnight at 4˚C. The slides were exposed to the EnVision secondary antibody reagent (DAKO, Tokyo, Japan). The color development was performed using a DAB Peroxidase Substrate Kit (Vector Laboratories, Burlingame, CA, USA), and the sections were counterstained with hematoxylin. GPX4 expression in GC cells was evaluated in a blinded manner, and a two-tiered discrimination using positive or negative staining was used. Tumors with >25% positive

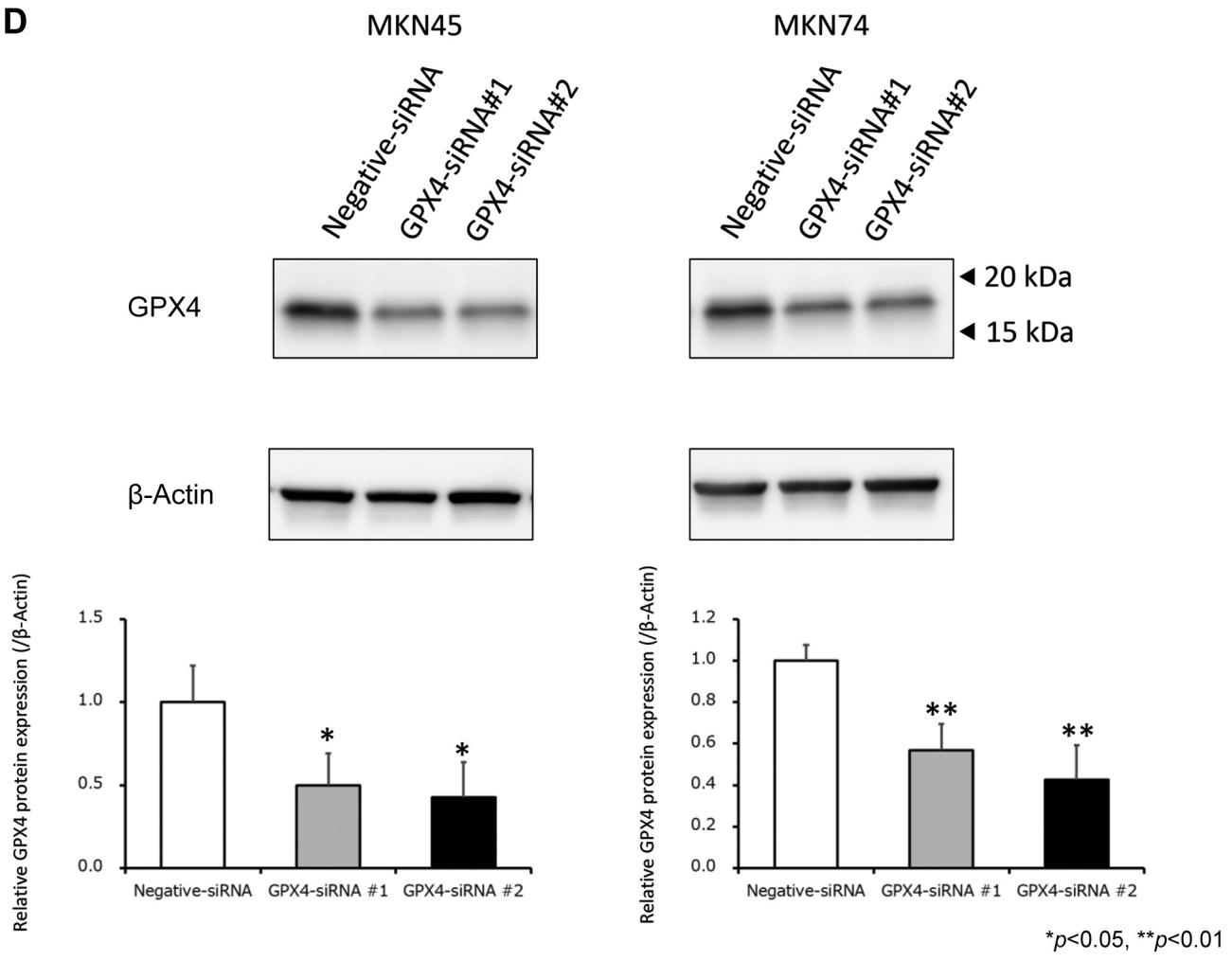

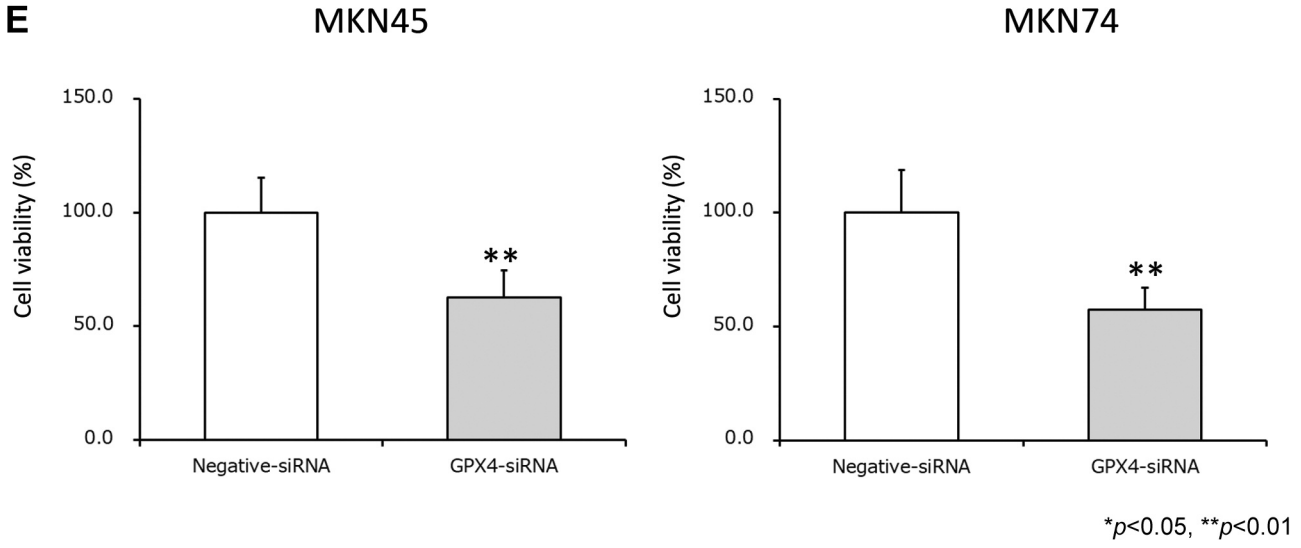

Figure 1. *Continued*

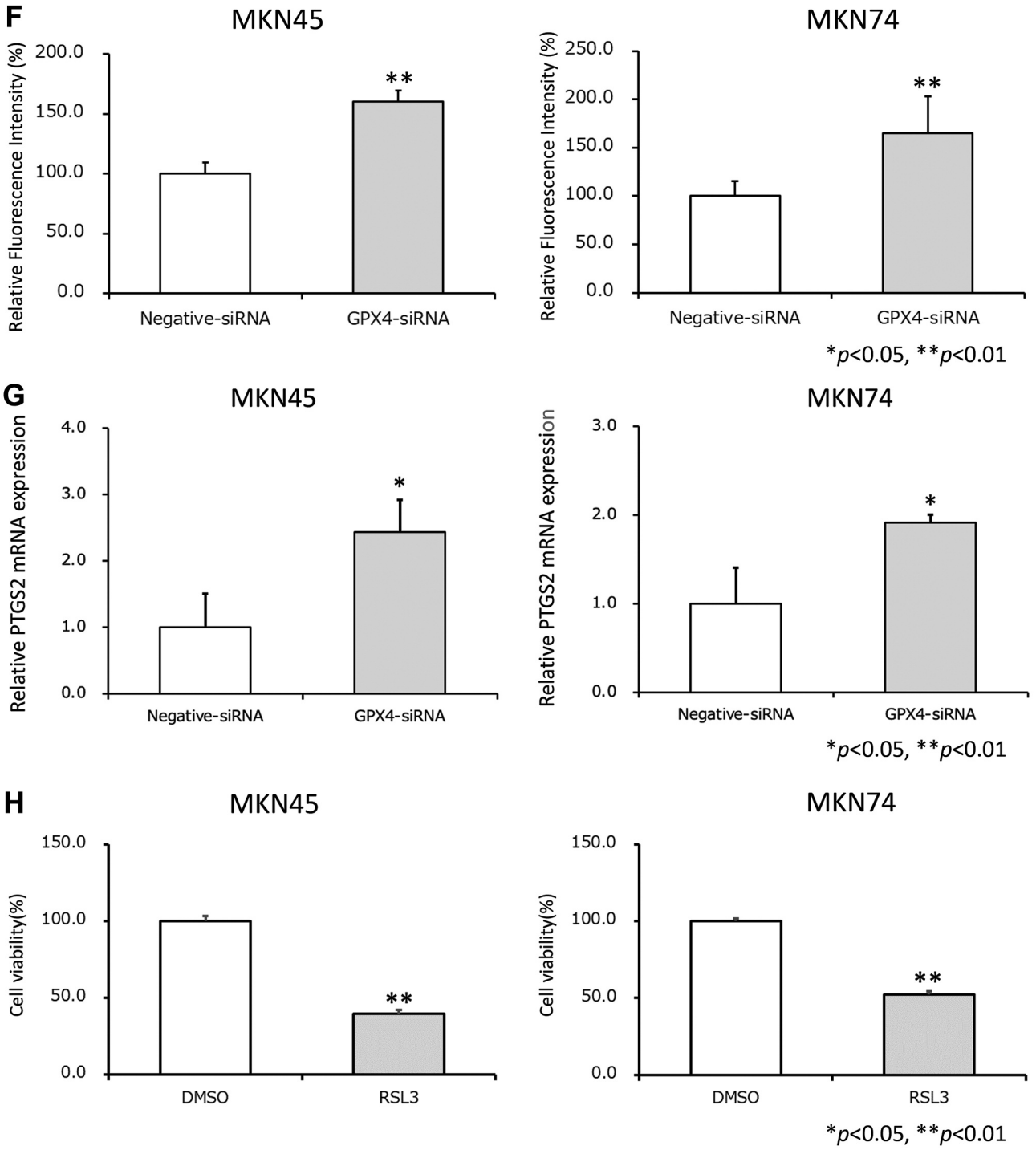

Figure 1. *Continued*

cells were classified as having high expression, and those with ≤25% positive cells were classified as having low expression. Two investigators (K.S. and M.M.) evaluated the immunolabeling; agreement was obtained in each case.

Statistical analysis. Univariate analyses were performed using two-tailed *t*-tests for continuous variables. Kruskal-Wallis test was used as a non-parametric test for estimating the differences between three or more groups. The Kaplan-Meier method was used for survival

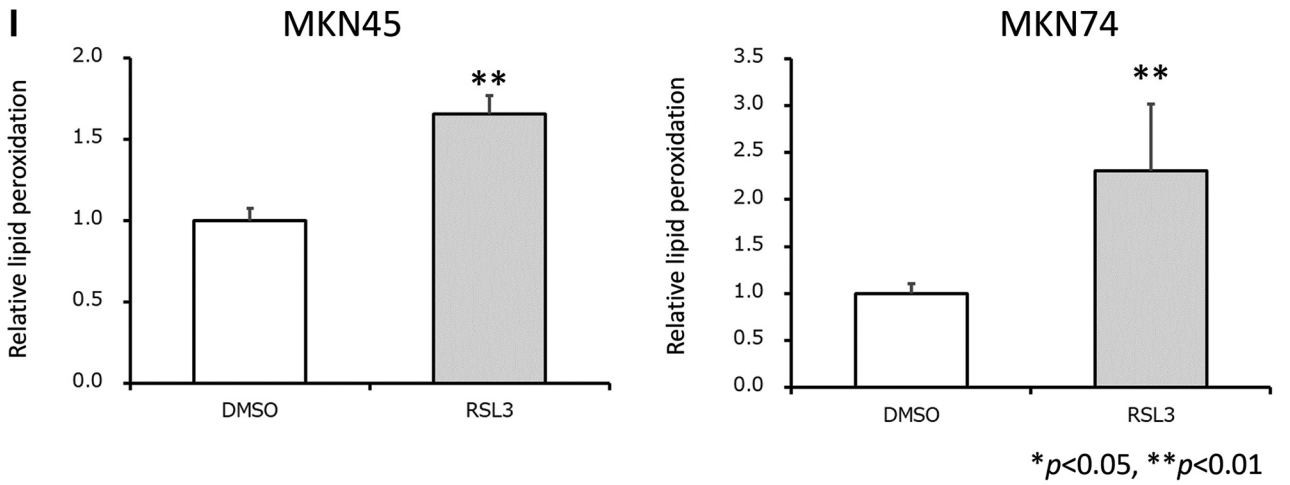

Figure 1. *GPX4 expression in gastric cancer (GC) cell lines and the effects of GPX4 silencing and inhibition. GPX4 expression in GC cell lines was analyzed using (A) real-time quantitative PCR and (B) western blotting. (C) Lipid peroxidation in GC cells was analyzed using flow cytometry. (D) GPX4 expression in GC cell lines was analyzed using western blotting 48 h after siRNA transfection. (E) The effect of silencing GPX4 on cell proliferation was assessed by the WST assay 72 h after siRNA transfection. (F) The effect of silencing GPX4 on reactive oxygen species (ROS) was assessed by a ROS assay 72 h after siRNA transfection. (G) PTGS2 expression in GC cell lines was analyzed using real-time quantitative PCR 72 h after siRNA transfection. (H) The effect of suppressing GPX4 on cell proliferation was assessed by the WST assay. Cells were treated with DMSO and RSL3 (10 μM) for 48 h. (I) The effect of suppressing GPX4 on cell lipid peroxidation was assessed by flow cytometry. Cells were treated with DMSO and RSL3 (10 μM) for 48 h. Results are expressed as means±standard deviation. *p<0.05; **p<0.01.*

curves, and the differences in survival curves were compared using the log-rank test. Cox proportional hazards models were used for the multivariate analysis. All statistical analyses were examined using EZR version 3.6.1 (Saitama Medical Center, Jichi Medical University, Saitama, Japan) (13), and *p*-values <0.05 were considered statistically significant.

Results

GPX4 expression and ROS activity in gastric cancer cell lines. To verify the expression levels of GPX4 in GC cells, we first analyzed the expression of GPX4 in five human GC cell lines (KATO-III, MKN-1, MKN-28, MKN-45, and MKN-74) by RT-qPCR and western blot. GPX4 was expressed in each GC cell line at various levels (Figure 1A and B). Next, we examined the relative ROS activity using flow cytometry (Figure 1C). Interestingly, the cell lines with higher GPX4 expression (MKN-45 and MKN-74) had relatively lower ROS activity than those with lower GPX4 expression (MKN-1, MKN-28 and KATOIII). This suggests that GPX4 in gastric cancer has a role in the regulation of ferroptosis. For subsequent experiments, MKN-45 and MKN-74 cells were used because of the highest GPX4 expression levels.

Effect of silencing and inhibiting GPX4 in GC cells in vitro. To directly assess the role of GPX4 expression in GC cell lines, we performed GPX4 knockdown using siRNAs in MKN-45 and MKN-74 cells (Figure 1D) and confirmed the effect of GPX4 on tumor growth. The effect of GPX4 knockdown on cell proliferation was assessed by WST assay. Knockdown of GPX4 significantly reduced the number of cells compared with that in the control group at 72 h after silencing (Figure 1E).

GPX4 is known to be a regulator of ferroptosis, a type of cell death caused by the accumulation of lipid peroxides. We evaluated the effect of GPX4 depletion on ROS generation to clarify the mechanism by which growth inhibition may have occurred. Knockdown of GPX4 in MKN-45 and MKN-74 cells induced a significant increase in ROS levels at 72 h (Figure 1F). In addition, the mRNA level of PTGS2, a known biomarker of ferroptosis, was increased after GPX4 knockdown compared with that in control cells (Figure 1G). To confirm the GPX4 role in ferroptosis based on the siRNA experiments, we evaluated the efficacy of RSL3, a GPX4 inhibitor. Indeed, RSL3 inhibited cell proliferation and increased ROS activity in MKN-45 and MKN-74 cells (Figure 1H and I). Taken together, these results demonstrated an association between GPX4 down-regulation and induction of ferroptosis in GC cells.

GPX4 expression is negatively correlated with prognosis in GC patients. Based on the *in vitro* studies described above, we retrospectively analyzed the records and specimens of 106 GC patients who underwent gastrectomy to determine the importance of GPX4 expression in these patients. GPX4 positive staining was predominantly observed in the

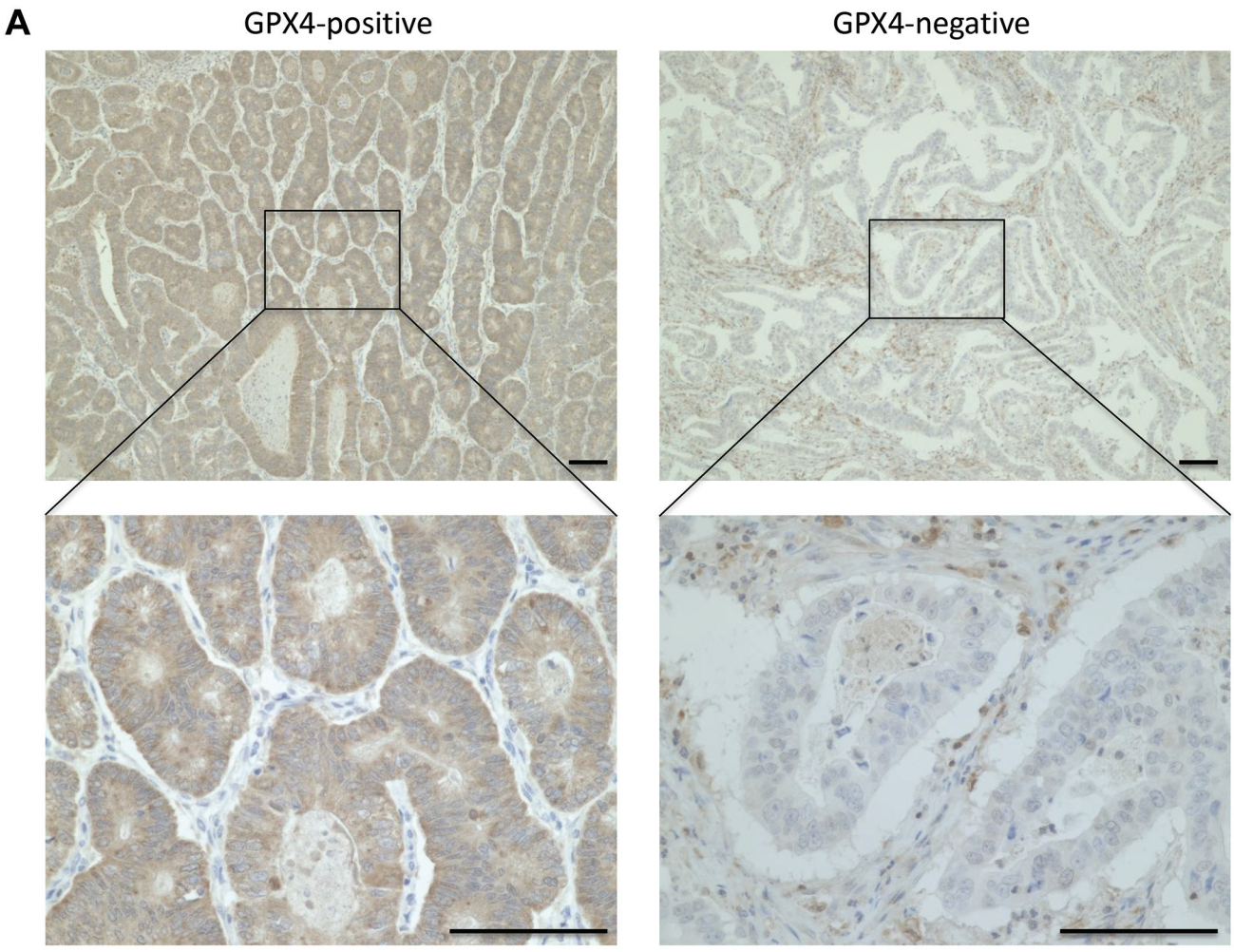

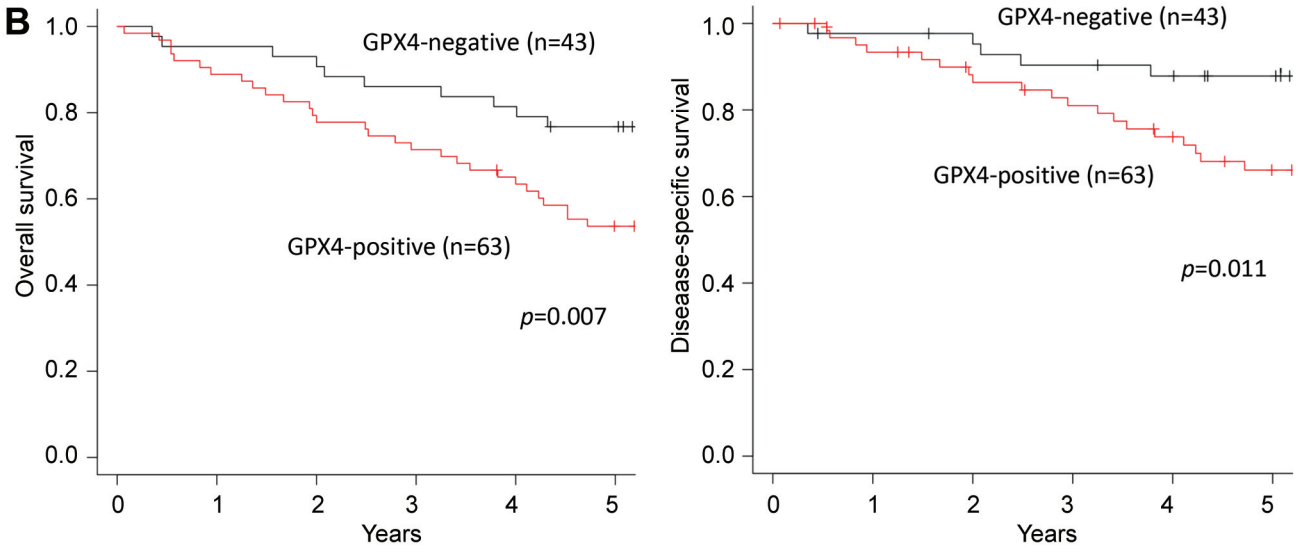

Figure 2. *GPX4 expression in gastric cancer (GC) tissues is negatively correlated with prognosis. (A) Representative images of GC tissue samples immunohistochemically stained for GPX4. Scale bar: 100 μm. (B) Correlation between GPX4 expression and prognosis using the Kaplan-Meier method.*

Table I. *Association between GPX4 expression and clinicopathological factors.*

Parameter	GPX4 expression, n (%)		*p*-Value
	Negative n=43	Positive n=63	
Age			
<65 Years	13 (38.2)	21 (61.8)	0.83
≥65 Years	30 (41.7)	42 (58.3)	
Sex			
Male	31 (39.8)	49 (61.2)	0.65
Female	12 (46.2)	14 (53.8)	
BMI			
<25 Kg/m^2	36 (40)	54 (60)	0.79
≥25 Kg/m^2	7 (43.8)	9 (56.2)	
Neoadjuvant chemotherapy			
Yes	3 (60)	2 (40)	0.39
No	40 (39.6)	61 (60.4)	
Adjuvant chemotherapy			
Yes	20 (45.5)	24 (54.5)	0.43
No	23 (37.1)	39 (62.9)	
Stage			
II	30 (42.3)	41 (57.7)	0.68
III	13 (37.1)	22 (62.9)	
Histologic type			
Well	22 (40)	33 (60)	1
Mod/poor	21 (41.2)	30 (58.8)	
Vascular invasion			
Negative	4 (57.1)	3 (42.9)	0.44
Positive	39 (39.4)	60 (60.6)	
Lymphatic invasion			
Negative	1 (100)	0 (0)	0.41
Positive	42 (40)	63 (60)	
pT			
I/II	11 (52.4)	10 (47.6)	0.23
III/IV	32 (37.6)	53 (62.4)	
pN			
Negative	13 (38.2)	21 (61.8)	0.83
Positive	30 (41.7)	42 (58.3)	
CEA			
<5 ng/ml	32 (38.1)	52 (61.9)	0.13
≥5 ng/ml	11 (57.9)	8 (42.1)	
CA19-9			
<37 U/ml	38 (42.2)	52 (57.8)	1
≥37 U/ml	5 (38.5)	8 (61.5)	

BMI: Body mass index; pN: pathological N classification; pT: pathological T classification; CEA: carcinoembryonic antigen; CA19-9: carbohydrate antigen 19-9.

cytoplasm of cancer cells (Figure 2A). After analyzing the expression of GPX4 in surgically resected specimens using immunohistochemistry, we found that 63 out of 106 patients (59.4%) were positive for GPX4 expression (Table I). There was no correlation between GPX4 expression and each of the clinicopathological factors examined (Table II).

Next, we investigated whether GPX4 expression played a role as a prognostic factor for GC patients. Kaplan-Meier survival analysis showed that GC patients with GPX4-positive tumors had significantly worse OS (p=0.007) and lower disease-specific survival (DSS; p=0.011) than patients with GPX4-negative tumors (Figure 2B). In the univariate analysis of the Cox proportional hazards model for OS, age ≥65 years, stage III disease, CA19-9 ≥37 U/ml, and positive expression of GPX4 were selected as significant risk factors. Multivariate analysis of these factors indicated that age ≥65 years, stage III disease, and positive expression of GPX4 were independent prognostic factors for OS. In the univariate analysis for DSS, stage III disease and positive GPX4 expression were also risk factors, and these factors were independent prognostic factors for DSS in the multivariate analysis (Table III). The results of these studies indicated that GPX4 over-expression is a significant negative prognostic factor for GC patients.

Discussion

Apoptosis was the first type of regulated programmed cell death that was identified at the molecular level followed by autophagy and necroptosis. In recent years, there has been a growing interest in the importance of other regulated cell death systems beyond apoptosis that can explain the mechanisms of tumorigenesis and efficacy of anti-cancer treatments (14, 15). Ferroptosis is a form of regulated cell death characterized by the iron-dependent accumulation of lethal levels of lipid hydroperoxides (16), which originate from polyunsaturated fatty acids in plasma membranes and result in the rupture of cellular membranes. Ferroptotic cell death is caused by the production of both cytosolic and lipid ROS and is independent of mitochondria but dependent on NADPH oxidases (17). Unlike apoptosis and necroptosis, cells dying by ferroptosis primarily exhibit shrunken and damaged mitochondria with few other morphological changes evident prior to death (18).

Recently, ferroptosis investigations have focused on the mechanisms of tumor cell killing by ferroptosis-inducing agents and the promotion of tumor progression by the abnormal inhibition of ferroptosis. Yang *et al*. reported that the small molecule erastin inhibited the import of cysteine *via* the cystine/glutamate antiporter system xc$^-$, which resulted in glutathione depletion and inactivation of GPX4 (19). Furthermore, it was revealed that induction of ferroptosis reduced the growth of subcutaneously xenografted tumors derived from the human foreskin fibroblast cell line BJeLR (5). Thus, the GPX4-glutathione-cysteine axis and GPX4-associated lipid peroxidation are known to be central regulators of ferroptosis and may represent potential cancer therapeutic targets. Lu *et al*. showed that migration and invasion by clear cell renal cell carcinoma (ccRCC) cells was repressed by the inhibition of GPX4 and subsequent upregulation of

Table II. *Univariate and multivariate analyses of prognostic factors associated with overall survival.*

	Univariate analysis			Multivariate analysis		
	HR	95%CI	*p*-Value	HR	95%CI	*p*-Value
Age (<65 *vs.* ≥65)	2.651	1.284-5.473	0.008*	2.503	1.143-5.485	0.022*
Sex (Female *vs.* Male)	1.193	0.6099-2.335	0.61			
BMI (<25 *vs.* ≥25)	0.5934	0.2352-1.497	0.27			
Neoadjuvant chemotherapy (No *vs.* Yes)	2.045	0.7345-5.693	0.17			
Adjuvant chemotherapy (No *vs.* Yes)	0.9482	0.5358-1.678	0.86			
Stage (II *vs.* III)	2.098	1.193-3.691	0.01*	1.881	1.032-3.427	0.039*
Histology (Well *vs.* Mod/poor)	1.003	0.5723-1.759	0.99			
pT (I-II *vs.* III-IV)	0.9823	0.4765-2.025	0.96			
pN (Negative *vs.* Positive)	1.495	0.7927-2.821	0.21			
CEA (<5 *vs.* ≥5)	1.412	0.7005-2.847	0.33			
CA19-9 (<37 *vs.* ≥37)	2.198	1.087-4.444	0.028*	1.447	0.687-3.047	0.33
GPX4 (Negative *vs.* Positive)	2.326	1.232-4.392	0.009*	2.23	1.171-4.244	0.015*

HR: Hazard ratio; CI: confidence interval; BMI: body mass index; pN: pathological N classification; pT: pathological T classification; CEA: carcinoembryonic antigen; CA19-9: carbohydrate antigen 19-9. *Statistically significant.

Table III. *Univariate and multivariate analyses of prognostic factors associated with disease-specific survival.*

	Univariate analysis			Multivariate analysis		
	HR	95%CI	*p*-Value	HR	95%CI	*p*-Value
Age (<65 *vs.* ≥65)	1.464	0.643-3.332	0.36			
Sex (Female *vs.* Male)	2.854	0.8615-9.454	0.085			
BMI (<25 *vs.* ≥25)	0.1906	0.0259-1.403	0.1			
Neoadjuvant chemotherapy (No *vs.* Yes)	1.744	0.4134-7.358	0.45			
Adjuvant chemotherapy (No *vs.* Yes)	1.591	0.7557-3.348	0.22			
Stage (II *vs.* III)	2.553	1.215-5.368	0.013*	2.476	1.177-5.208	0.017*
Histology (Well *vs.* Mod/poor)	0.7515	0.3518-1.605	0.46			
pT (I-II *vs.* III-IV)	0.8219	0.3331-2.028	0.67			
pN (Negative *vs.* Positive)	1.282	0.903-1.82	0.16			
CEA (<5 *vs.* ≥5)	1.62	0.6467-4.059	0.3			
CA19-9 (<37 *vs.* ≥37)	2.011	0.7505-5.389	0.16			
GPX4 (Negative *vs.* Positive)	3.064	1.24-7.57	0.015*	2.981	1.206-7.369	0.018*

HR: Hazard ratio; CI: confidence interval; BMI: body mass index; pN: pathological N classification; pT: pathological T classification; CEA: carcinoembryonic antigen; CA19-9: carbohydrate antigen 19-9. *Statistically significant.

ferroptosis (20). *In vitro*, it was reported that expression of GPX4 increased the proliferation of oral cancer cells (21). One study also reported that GPX4 was involved in ccRCC and ovarian cancer cell morphology, and a GPX4-dependent cancer cell state conferred sensitivity to ferroptosis, which is potentially translatable toward novel therapies that inhibit GPX4 (22). Another study reported that miR-15a-3p suppressed colorectal cancer cell growth and enhanced ferroptosis by inactivating GPX4 (23). These data support the hypothesis that the regulation of ferroptosis *via* GPX4 plays an important role in cancer progression. Consistent with this hypothesis, our results revealed that GPX4 silencing suppressed tumor progression and promoted ROS production, which induced ferroptosis in GC cell lines.

There are a few studies which attempted to prove the correlation between the prognosis in patients with GC and GPX4 (24, 25). However, the prognostic property was inconsistently reported in each study and there is no consensus on the role of GPX4 in gastric cancer progression at the cellular level yet.

Various molecules have been discovered and studied that clarify the mechanisms regulating ferroptosis and implicate potential strategies for cancer treatment. For example, in addition to GPX4, NRF2, p53, and ferroptosis suppressor protein 1 (FSP1), also known as apoptosis inducing factor

mitochondrial associated 2, have been studied as key regulators of ferroptosis (26). NRF2 expression in GC was reported to be associated with aggressive tumor behavior (27). The tumor suppressor *TP53* is the most frequently mutated gene in human cancers, and it has been reported that 59% of GC patients have tumors with mutated *TP53* (28). Recently, FSP1 was reported as a key component of a non-mitochondrial CoQ antioxidant system that acts in parallel to the canonical glutathione-based GPX4 pathway (29). In the present study, the expression of GPX4 in cancer cell lines and tumor tissue from patients with GC and its regulatory role in ferroptosis were confirmed. Taken together, these data suggest that GC progression may involve the inhibition of ferroptosis *via* p53, FSP1, and GPX4.

In the present study, we have confirmed GPX4 expression in GC cell lines at both the protein and mRNA levels. Furthermore, suppression of GPX4 expression inhibited cell proliferation and induced ROS production in MKN-45 and MKN-74 cell lines. Additionally, GPX4 silencing significantly increased the expression of PTGS2 mRNA, which is a marker of ferroptosis. RSL3 reduced cell viability and increased lipid peroxidation in MKN-45 and MKN-74. The silencing and pharmacological inhibition of GPX4 indicated that GPX4 plays a great role in GC cells *via* ferroptosis suppression and can be a therapeutic target of GC. Finally, we demonstrated that positive expression of GPX4 protein in surgically resected tumor specimens from patients with GC was an independent risk factor for postoperative survival. These results suggest that GPX4 may be one of the key molecules that promotes GC progression through inhibition of ferroptosis. Thus, regulating ferroptosis has become an emerging novel strategy for cancer treatment and includes the development of ferroptosis-inducing chemotherapeutic agents.

Conflicts of Interest

The Authors have no conflicts of interest or financial ties to disclose in relation to this study.

Authors' Contributions

KS, MM, MY, YN and YM established the study design and analytical concept. KS and MM performed statistical analyses and drafted the manuscript. KS, KH, CU, and KK contributed to the acquisition of clinical data. KS and MM contributed to writing the manuscript. MM, TM, NT, TS, YU, and YF made critical revisions of the manuscript. All Authors have read and approved the manuscript.

Acknowledgements

The Authors thank Susan Zunino, Ph.D., from Edanz (https://jp.edanz.com/ac) for editing a draft of this manuscript.

References

1 Sung H, Ferlay J, Siegel RL, Laversanne M, Soerjomataram I, Jemal A and Bray F: Global cancer statistics 2020: GLOBOCAN estimates of incidence and mortality worldwide for 36 cancers in 185 countries. CA Cancer J Clin *71(3)*: 209-249, 2021. PMID: 33538338. DOI: 10.3322/caac.21660

2 Katai H, Ishikawa T, Akazawa K, Isobe Y, Miyashiro I, Oda I, Tsujitani S, Ono H, Tanabe S, Fukagawa T, Nunobe S, Kakeji Y, Nashimoto A and Registration Committee of the Japanese Gastric Cancer Association: Five-year survival analysis of surgically resected gastric cancer cases in Japan: a retrospective analysis of more than 100,000 patients from the nationwide registry of the Japanese Gastric Cancer Association (2001-2007). Gastric Cancer *21(1)*: 144-154, 2018. PMID: 28417260. DOI: 10.1007/s10120-017-0716-7

3 Imai H and Nakagawa Y: Biological significance of phospholipid hydroperoxide glutathione peroxidase (PHGPx, GPx4) in mammalian cells. Free Radic Biol Med *34(2)*: 145-169, 2003. PMID: 12521597. DOI: 10.1016/s0891-5849(02)01197-8

4 Hanahan D and Weinberg RA: Hallmarks of cancer: the next generation. Cell *144(5)*: 646-674, 2011. PMID: 21376230. DOI: 10.1016/j.cell.2011.02.013

5 Yang WS, SriRamaratnam R, Welsch ME, Shimada K, Skouta R, Viswanathan VS, Cheah JH, Clemons PA, Shamji AF, Clish CB, Brown LM, Girotti AW, Cornish VW, Schreiber SL and Stockwell BR: Regulation of ferroptotic cancer cell death by GPX4. Cell *156(1-2)*: 317-331, 2014. PMID: 24439385. DOI: 10.1016/j.cell.2013.12.010

6 Guerriero E, Capone F, Accardo M, Sorice A, Costantini M, Colonna G, Castello G and Costantini S: GPX4 and GPX7 over-expression in human hepatocellular carcinoma tissues. Eur J Histochem *59(4)*: 2540, 2015. PMID: 26708178. DOI: 10.4081/ejh.2015.2540

7 Yagublu V, Arthur JR, Babayeva SN, Nicol F, Post S and Keese M: Expression of selenium-containing proteins in human colon carcinoma tissue. Anticancer Res *31(9)*: 2693-2698, 2011. PMID: 21868509.

8 Cejas P, García-Cabezas MA, Casado E, Belda-Iniesta C, De Castro J, Fresno JA, Sereno M, Barriuso J, Espinosa E, Zamora P, Feliu J, Redondo A, Hardisson DA, Renart J and González-Barón M: Phospholipid hydroperoxide glutathione peroxidase (PHGPx) expression is downregulated in poorly differentiated breast invasive ductal carcinoma. Free Radic Res *41(6)*: 681-687, 2007. PMID: 17516241. DOI: 10.1080/10715760701286167

9 Rudenko E, Kondratov O, Gerashchenko G, Lapska Y, Kravchenko S, Koliada O, Vozianov S, Zgonnyk Y and Kashuba V: Aberrant expression of selenium-containing glutathione peroxidases in clear cell renal cell carcinomas. Exp Oncol *37(2)*: 105-110, 2015. PMID: 26112936.

10 Kinowaki Y, Kurata M, Ishibashi S, Ikeda M, Tatsuzawa A, Yamamoto M, Miura O, Kitagawa M and Yamamoto K: Glutathione peroxidase 4 overexpression inhibits ROS-induced cell death in diffuse large B-cell lymphoma. Lab Invest *98(5)*: 609-619, 2018. PMID: 29463878. DOI: 10.1038/s41374-017-0008-1

11 Liu K, Jin M, Xiao L, Liu H and Wei S: Distinct prognostic values of mRNA expression of glutathione peroxidases in non-

small cell lung cancer. Cancer Manag Res *10*: 2997-3005, 2018. PMID: 30214294. DOI: 10.2147/CMAR.S163432

12 Shishido Y, Amisaki M, Matsumi Y, Yakura H, Nakayama Y, Miyauchi W, Miyatani K, Matsunaga T, Hanaki T, Kihara K, Yamamoto M, Tokuyasu N, Takano S, Sakamoto T, Honjo S, Hasegawa T and Fujiwara Y: Antitumor effect of 5-aminolevulinic acid through ferroptosis in esophageal squamous cell carcinoma. Ann Surg Oncol *28(7)*: 3996-4006, 2021. PMID: 33210267. DOI: 10.1245/s10434-020-09334-4

13 Kanda Y: Investigation of the freely available easy-to-use software 'EZR' for medical statistics. Bone Marrow Transplant *48(3)*: 452-458, 2013. PMID: 23208313. DOI: 10.1038/bmt.2012.244

14 Tang D, Lotze MT, Kang R and Zeh HJ: Apoptosis promotes early tumorigenesis. Oncogene *30(16)*: 1851-1854, 2011. PMID: 21151175. DOI: 10.1038/onc.2010.573

15 Mocellin S, Rossi CR, Pilati P and Nitti D: Tumor necrosis factor, cancer and anticancer therapy. Cytokine Growth Factor Rev *16(1)*: 35-53, 2005. PMID: 15733831. DOI: 10.1016/j.cytogfr.2004.11.001

16 Stockwell BR, Friedmann Angeli JP, Bayir H, Bush AI, Conrad M, Dixon SJ, Fulda S, Gascón S, Hatzios SK, Kagan VE, Noel K, Jiang X, Linkermann A, Murphy ME, Overholtzer M, Oyagi A, Pagnussat GC, Park J, Ran Q, Rosenfeld CS, Salnikow K, Tang D, Torti FM, Torti SV, Toyokuni S, Woerpel KA and Zhang DD: Ferroptosis: a regulated cell death nexus linking metabolism, redox biology, and disease. Cell *171(2)*: 273-285, 2017. PMID: 28985560. DOI: 10.1016/j.cell.2017.09.021

17 Dixon SJ, Lemberg KM, Lamprecht MR, Skouta R, Zaitsev EM, Gleason CE, Patel DN, Bauer AJ, Cantley AM, Yang WS, Morrison B 3rd and Stockwell BR: Ferroptosis: an iron-dependent form of nonapoptotic cell death. Cell *149(5)*: 1060-1072, 2012. PMID: 22632970. DOI: 10.1016/j.cell.2012.03.042

18 Abrams RP, Carroll WL and Woerpel KA: Five-membered ring peroxide selectively initiates ferroptosis in cancer cells. ACS Chem Biol *11(5)*: 1305-1312, 2016. PMID: 26797166. DOI: 10.1021/acschembio.5b00900

19 Yang WS and Stockwell BR: Ferroptosis: Death by lipid peroxidation. Trends Cell Biol *26(3)*: 165-176, 2016. PMID: 26653790. DOI: 10.1016/j.tcb.2015.10.014

20 Lu Y, Qin H, Jiang B, Lu W, Hao J, Cao W, Du L, Chen W, Zhao X and Guo H: KLF2 inhibits cancer cell migration and invasion by regulating ferroptosis through GPX4 in clear cell renal cell carcinoma. Cancer Lett *522*: 1-13, 2021. PMID: 34520818. DOI: 10.1016/j.canlet.2021.09.014

21 Fukuda M, Ogasawara Y, Hayashi H, Okuyama A, Shiono J, Inoue K and Sakashita H: Down-regulation of glutathione peroxidase 4 in oral cancer inhibits tumor growth through SREBP1 signaling. Anticancer Res *41(4)*: 1785-1792, 2021. PMID: 33813383. DOI: 10.21873/anticanres.14944

22 Zou Y, Palte MJ, Deik AA, Li H, Eaton JK, Wang W, Tseng YY, Deasy R, Kost-Alimova M, Dančík V, Leshchiner ES, Viswanathan VS, Signoretti S, Choueiri TK, Boehm JS, Wagner BK, Doench JG, Clish CB, Clemons PA and Schreiber SL: A GPX4-dependent cancer cell state underlies the clear-cell morphology and confers sensitivity to ferroptosis. Nat Commun *10(1)*: 1617, 2019. PMID: 30962421. DOI: 10.1038/s41467-019-09277-9

23 Liu L, Yao H, Zhou X, Chen J, Chen G, Shi X, Wu G, Zhou G and He S: MiR-15a-3p regulates ferroptosis *via* targeting glutathione peroxidase GPX4 in colorectal cancer. Mol Carcinog *61(3)*: 301-310, 2022. PMID: 34727409. DOI: 10.1002/mc.23367

24 Ouyang S, Li H, Lou L, Huang Q, Zhang Z, Mo J, Li M, Lu J, Zhu K, Chu Y, Ding W, Zhu J, Lin Z, Zhong L, Wang J, Yue P, Turkson J, Liu P, Wang Y and Zhang X: Inhibition of STAT3-ferroptosis negative regulatory axis suppresses tumor growth and alleviates chemoresistance in gastric cancer. Redox Biol *52*: 102317, 2022. PMID: 35483272. DOI: 10.1016/j.redox.2022.102317

25 Zhao L, Peng Y, He S, Li R, Wang Z, Huang J, Lei X, Li G and Ma Q: Apatinib induced ferroptosis by lipid peroxidation in gastric cancer. Gastric Cancer *24(3)*: 642-654, 2021. PMID: 33544270. DOI: 10.1007/s10120-021-01159-8

26 Shi Z, Zhang L, Zheng J, Sun H and Shao C: Ferroptosis: Biochemistry and biology in cancers. Front Oncol *11*: 579286, 2021. PMID: 33868986. DOI: 10.3389/fonc.2021.579286

27 Kawasaki Y, Ishigami S, Arigami T, Uenosono Y, Yanagita S, Uchikado Y, Kita Y, Nishizono Y, Okumura H, Nakajo A, Kijima Y, Maemura K and Natsugoe S: Clinicopathological significance of nuclear factor (erythroid-2)-related factor 2 (Nrf2) expression in gastric cancer. BMC Cancer *15*: 5, 2015. PMID: 25588809. DOI: 10.1186/s12885-015-1008-4

28 Cai H, Jing C, Chang X, Ding D, Han T, Yang J, Lu Z, Hu X, Liu Z, Wang J, Shang L, Wu S, Meng P, Lin L, Zhao J, Nie M and Yin K: Mutational landscape of gastric cancer and clinical application of genomic profiling based on target next-generation sequencing. J Transl Med *17(1)*: 189, 2019. PMID: 31164161. DOI: 10.1186/s12967-019-1941-0

29 Bersuker K, Hendricks JM, Li Z, Magtanong L, Ford B, Tang PH, Roberts MA, Tong B, Maimone TJ, Zoncu R, Bassik MC, Nomura DK, Dixon SJ and Olzmann JA: The CoQ oxidoreductase FSP1 acts parallel to GPX4 to inhibit ferroptosis. Nature *575(7784)*: 688-692, 2019. PMID: 31634900. DOI: 10.1038/s41586-019-1705-2

Received September 22, 2022
Revised September 29, 2022
Accepted September 30, 2022